

# Autostereoscopic 3D projection display based on two lenticular sheets

Lin Qi (祁 林)<sup>1</sup>, Qionghua Wang (王琼华)<sup>1,2\*</sup>, Jiangyong Luo (罗江勇)<sup>1</sup>,  
Aihong Wang(王爱红)<sup>1</sup>, and Dong Liang (梁 栋)<sup>1</sup>

<sup>1</sup>School of Electronics and Information Engineering, Sichuan University, Chengdu 610065, China

<sup>2</sup>State Key Laboratory of Fundamental Science on Synthetic Vision, Sichuan University, Chengdu 610065, China

\*Corresponding author: qhwang@scu.edu.cn

Received March 24, 2011; accepted May 19, 2011; posted online August 5, 2011

We propose an autostereoscopic three-dimensional (3D) projection display. The display consists of four projectors, a projection screen, and two lenticular sheets. The operation principle and calculation equations are described in detail and the parallax images are corrected by means of homography. A 50-inch autostereoscopic 3D projection display prototype is developed. The normalized luminance distributions of viewing zones from the simulation and the measurement are given. Results agree well with the designed values. The proposed prototype presents full-resolution 3D images similar to the conventional prototype based on two parallax barriers. Moreover, the proposed prototype shows considerably higher brightness and efficiency of light utilization.

OCIS codes: 110.0110, 110.6880.

doi: 10.3788/COL201210.011101.

Three-dimensional (3D) displays, which offer the viewer the realism lacking in conventional two-dimensional (2D) displays, are candidates for next-generation image media<sup>[1,2]</sup>. Currently, various types of 3D displays are both available and under development. Traditional technologies use classical 2-view stereo with one view for each eye and a kind of glasses to filter the corresponding view into each eye. Such stereoscopic displays rely on color separation, polarization, or shutter technology<sup>[3–5]</sup>. Stereoscopic displays have reached a certain level of maturity and are readily available for professional and private users.

Multi-view autostereoscopic displays are advanced systems that do not require glasses<sup>[6–8]</sup>. An autostereoscopic display consists of a 2D display and a lenticular sheet or a parallax barrier. For an  $N$ -view autostereoscopic display,  $N$  different parallax images are displayed on the 2D display at the same time and a lenticular sheet or parallax barrier in front of the 2D display ensures correct view separation for the eyes of the viewer. The resolution of each single view is inversely proportional to  $N$ . The size of the 2D display is limited, hence, it is difficult to realize large-screen and high-resolution 3D display. However, 3D projection display is an effective approach to realizing large-screen and high-resolution 3D display. In the past several years, several types of 3D projection displays have been proposed to achieve high-resolution images<sup>[9,10]</sup>.

A 3D projection display based on two parallax barriers which present full-resolution 3D images has been developed<sup>[10]</sup>. However, most of the light from the projectors is blocked by two parallax barriers. Considerable light energy is lost and the brightness of the 3D projection display is lowered. In this letter, we propose an autostereoscopic 3D projection display based on two lenticular sheets which consequently increase the brightness of the display.

The proposed autostereoscopic 3D projection display

consists of four projectors, a projection screen, and two lenticular sheets, as shown in Fig. 1. Four projectors are arranged in a horizontal array and they project four parallax images onto the lenticular sheet. The projected parallax images pass through lenticular sheet 1 facing the projectors and form a synthetic image on the projection screen. The synthetic image includes four parallax images, which are vertically interlaced. Lenticular sheet 2, which is between the projection screen and the viewer, ensures correct parallax image separation for the left and right eyes of the viewer.

In Fig. 1, the pitch and the focal length of lenticular sheet 1 are denoted by  $P_1$  and  $F$ , respectively. The focal plane is located at the back plane surface of lenticular sheet 1.  $H_1$  and  $H_2$  are the principal planes of lenticular sheet 1.  $L$  is the projection distance. Assuming that the incident rays passing through each lenticular lens are parallel, the pitch of the lenticular sheet  $P_1$  is far less than the projection distance  $L$ . Based on the principle of geometry optics, projection lights from a projector pass through the lenticular sheet and form a set of equidistant focuses. The focus position entirely depends on the horizontal position of the projector. When the distance between every two adjacent projectors  $E$  satisfies

$$E = \frac{L + F}{5F} P_1, \quad (1)$$

parallax images from four projectors pass through lenticular sheet 1 and form a synthetic image on the projection screen. According to the geometric analysis, the distance between lenticular sheet 1 and the projection screen is  $D$ , which can be obtained by

$$\frac{D}{D + F} = \frac{1}{5} \left( 1 + \frac{F}{L} \right), \quad (2)$$

The pixel pitch of the synthetic image is denoted by  $p$ , which can be calculated from

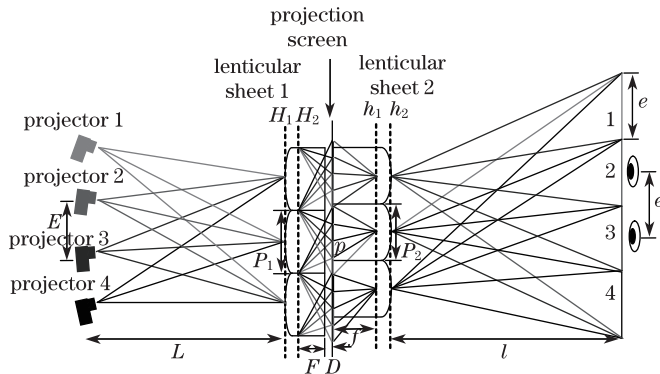


Fig. 1. Configuration of the proposed autostereoscopic 3D projection display.

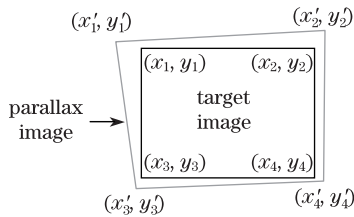


Fig. 2. Relative coordinates of the parallax image and its target image.

$$p = \frac{DP_1}{F}, \tag{3}$$

The projection screen is placed at the focal plane of lenticular sheet 2. The focal plane coincides with the back plane surface.  $h_1$  and  $h_2$  are the principal planes of lenticular sheet 2. The pitch and the focal length of lenticular sheet 2 are denoted by  $P_2$  and  $f$ , respectively. According to the geometric relations,  $P_2$  and  $f$  are obtained by

$$f = \frac{pl}{e}, \tag{4}$$

$$P_2 = \frac{4pe}{p + e}. \tag{5}$$

At the optimum viewing distance  $l$ , viewing zones 1, 2, 3, and 4 correspond with views projected from projectors 1, 2, 3, and 4, respectively. The width of a single viewing zone is  $e$ , which is equal to the interpupillary distance.

The four projectors in the autostereoscopic 3D projection display are placed at four places along the horizontal direction with horizontal shift. Moreover, the distance between every two adjacent projectors  $E$  should be limited by Eq. (1). If the width of each projector is larger than the value, the four projectors cannot be placed on one layer, which causes a vertical shift. The phenomenon leads to horizontal distortion and vertical parallax of the parallax images presented by the projectors. This degrades the stereoscopic effect and even causes serious eye fatigue<sup>[11]</sup>. Thus, correcting the parallax images is necessary.

We correct the parallax images by means of homography. Homography is an invertible transformation from one projective plane to another that maps straight lines to straight lines<sup>[12]</sup>. The geometric properties of images do not change before and after the transformation. The equations of homography are represented as

$$x' = \frac{ax + by + e}{ux + vy + 1}, \tag{6}$$

$$y' = \frac{cx + dy + f}{ux + vy + 1}, \tag{7}$$

where  $x$  and  $y$  are the coordinates of a point on a parallax image to be corrected,  $x'$  and  $y'$  are the coordinates of a point on the rectangular target image, and  $a, b, c, d, e, f, u,$  and  $v$  are the factors that can be obtained by four pairs of vertexes  $(x'_1, y'_1), (x_1, y_1), (x'_2, y'_2), (x_2, y_2), (x'_3, y'_3), (x_3, y_3), (x'_4, y'_4), (x_4, y_4)$ . These are shown in Fig. 2. All points on the parallax image are transformed to the rectangular target image, according to Eqs. (6) and (7). This process is called pre-transformation. When the pre-transformed parallax images are projected onto the projection screen, they overlap completely and have no vertical parallax and image deformation.

For a multi-view autostereoscopic display, different parallax images are first prepared for a stereoscopic image. Parallax images for the proposed projection prototype are captured by 3DMAX software, as shown in Fig. 3.

A 50-inch autostereoscopic 3D projection display prototype based on two lenticular sheets is designed. This is shown in Fig. 4. The prototype presents good stereoscopic images. The specifications are listed in Table 1. Four parallax images with a resolution of  $1024 \times 768$  (pixels) pass through lenticular sheet 1 and form a synthetic image with a resolution of  $4096 \times 768$  (pixels). The resolution of the 3D image is similar to that of the parallax image, i.e.,  $1024 \times 768$  (pixels). As a result, full-resolution 3D images can be achieved using the proposed autostereoscopic 3D projection display. The 3D image resolution depends on the parallax image resolution.

The simulated luminance distribution characteristics of one viewing zone of the autostereoscopic



Fig. 3. Four parallax images for the proposed autostereoscopic 3D projection display prototype.



Fig. 4. 50-inch autostereoscopic 3D projection display prototype.

3D display prototype are shown in Fig. 5(a). Luminance distribution from the measurement can be obtained by turning on the corresponding projector with white image and turning off the others. Luminance is measured by moving an imaging photometer along the horizontal direction at the optimum 3D view distance, as shown in Fig. 5(b). Horizontal axis  $X$  represents the horizontal position at the optimum viewing distance. The viewing position corresponds to the display center when  $X$  is equal to 0. Luminance distributions from the simulation and the measurement show similar zone profiles, and the horizontal distance between peak positions of two adjacent viewing zones matches the designed value of  $e$ .

A coequal conventional autostereoscopic 3D display prototype based on two parallax barriers is developed

**Table 1. Specifications of the Proposed 3D Projection Display Prototype**

Parameter	Value (nm)
$L$	1700
$P_1$	0.976
$F$	2.914
$E$	114
$D$	0.727
$p$	0.243
$l$	2500
$e$	65
$P_2$	0.968
$f$	9.346

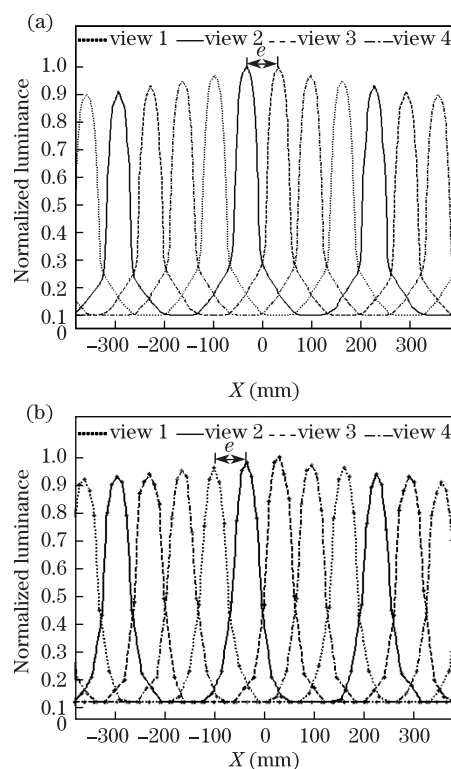


Fig. 5. Normalized luminance distribution of each viewing zone along the horizontal direction at the optimum viewing distance for the prototype, obtained from (a) the simulation and (b) the measurement.

**Table 2. Performances of Two Autostereoscopic 3D Projection Display Prototypes**

Performances	Proposed Prototype	Conventional Prototype
Screen Size (inch)	50	50
Brightness ( $\text{cd}/\text{m}^2$ )	827	153
Resolution of Parallax Image	$1024 \times 768$	$1024 \times 768$
Resolution of 3D Image	$1024 \times 768$	$1024 \times 768$
Optimum Viewing Distance (mm)	2500	2500

for comparison. The performance parameters of the two prototypes are shown in Table 2. Evidently, the proposed autostereoscopic 3D display prototype presents full-resolution 3D images in the same manner as the conventional prototype. More importantly, the brightness of the proposed prototype is nearly six times higher than that of the conventional prototype.

In conclusion, an autostereoscopic 3D projection display is proposed to realize 3D image with a large size and full-resolution. The operation principle and calculation equations are described in detail. A 50-inch autostereoscopic 3D projection display prototype, which is capable of presenting good stereoscopic images with full-resolution, is developed. Compared with the conventional autostereoscopic 3D projection display based on two parallax barriers, the proposed prototype has achieved higher brightness. The autostereoscopic 3D projection display has potential applications because of its many advantages, such as large size, full-resolution, and high luminance.

This work was supported by the National Natural Science Foundation of China under Grant Nos. 60877004 and 61036008.

## References

1. T. Kawai, *Displays* **23**, 49 (2002).
2. H. Yoshikawa and T. Yamaguchi, *Chin. Opt. Lett.* **7**, 1079 (2009).
3. A. J. Woods and C. R. Harris, *Proc. SPIE* **7253**, 0Q1 (2010).
4. H. Kang, S. D. Roh, I. S. Baik, H. J. Jung, W. N. Jeong, J. K. Shin, and I. J. Chung, *SID Symposium Digest of Technical Papers* **41**, 1 (2010).
5. J. C. Liou and F. G. Tseng, *Displays* **30**, 148 (2009).
6. Q. Wang, Y. Tao, W. Zhao, and D. Li, *Chin. Opt. Lett.* **8**, 22 (2010).
7. T. Yendo, T. Fujii, M. Tanimoto, and M. P. Tehrani, *J. Vis. Commun. Image R* **21**, 586 (2010).
8. X. Li, Q. Wang, Y. Tao, D. Li, and A. Wang, *Chin. Opt. Lett.* **9**, 021001 (2011).
9. J. S. Jang, Y. S. Oh, and B. Javidi, *Opt. Express* **12**, 557 (2004).
10. Y. H. Tao, Q. H. Wang, J. Gu, W. X. Zhao, and D. H. Li, *Opt. Lett.* **34**, 3220 (2009).
11. F. L. Kooi and A. Toet, *Displays* **25**, 99 (2004).
12. B. Zhang and Y. Li, *J. Opt. Soc. Am. A* **25**, 1389 (2008).